Acta Biomaterialia 11 (2015) 247–255

Contents lists available at ScienceDirect

Acta Biomaterialia

journal homepage: www.elsevier.com/locate/actabiomat

Linking naturally and unnaturally spun silks through the forced reeling of *Bombyx mori*

Beth Mortimer, Juan Guan [1], Chris Holland *, David Porter, Fritz Vollrath

University of Oxford, Department of Zoology, Oxford OX1 3PS, UK

ARTICLE INFO

Article history:
Received 12 May 2014
Received in revised form 18 August 2014
Accepted 12 September 2014
Available online 19 September 2014

Keywords:
Silk
Forced reeling
Postdraw
Glass transition
DMTA

ABSTRACT

The forced reeling of silkworms offers the potential to produce a spectrum of silk filaments, spun from natural silk dope and subjected to carefully controlled applied processing conditions. Here we demonstrate that the envelope of stress–strain properties for forced reeled silks can encompass both naturally spun cocoon silk and unnaturally processed artificial silk filaments. We use dynamic mechanical thermal analysis (DMTA) to quantify the structural properties of these silks. Using this well-established mechanical spectroscopic technique, we show high variation in the mechanical properties and the associated degree of disordered hydrogen-bonded structures in forced reeled silks. Furthermore, we show that this disorder can be manipulated by a range of processing conditions and even ameliorated under certain parameters, such as annealing under heat and mechanical load. We conclude that the powerful combination of forced reeling silk and DMTA has tied together native/natural and synthetic/unnatural extrusion spinning. The presented techniques therefore have the ability to define the potential of *Bombyx*-derived proteins for use in fibre-based applications and serve as a roadmap to improve fibre quality via post-processing.

1. Introduction

Silks are fibrous proteins spun by various arthropods for a variety of natural functions [1]. The silk of the mulberry silkworm *Bombyx mori* is of particular scientific interest, not least because its industrial-scale commercial production makes it an important model material for protein and polymer research [2]. The silks in their natural form are used by the silkworm to construct tough cocoons for protection during metamorphosis [3]. Using minimal specimen preparation, cocoon silk fibres can be unravelled from cocoons by softening them with water. The fibres themselves comprise two fibroin brins covered in a glue-like sericin coating, which can be further processed by removing the sericin and separating the brins in a process called degumming, which affects fibre mechanical properties [4].

These cocoon silk fibres are generally considered to be natural or native fibres, spun in vivo using natural protein dope feedstock. In contrast, "silk" fibres can also be spun artificially from reconstituted silk fibroin (RSF) protein molecules that have been obtained from native silks after dissolving in strong chaotropic agents [5,6]. Importantly for industrial uses, RSF can be processed in a number of ways to produce films, fibres, and a variety of 3-D structures, with a wide range of potential applications, principally for use in biomedical research [7–10].

Understanding the relationship between protein structure and mechanical properties is a vital step towards using silk or silk-derived proteins for specific applications. One of the most useful analytical tools allowing the matching of properties and structure is dynamic mechanical thermal analysis (DMTA), with detailed work to date helping to elucidate the protein structure of artificially produced fibroin [9,11–15], native silk fibres [16–19] and artificially spun fibres from natural silk dope [20–22]. This work has revealed differences in thermal behaviour between the different silk-derived proteins; most importantly, differences in glass transition temperatures (T_g) that can be linked to the degree of order in the protein, which in turn is a key component of protein structure determining mechanical performance [18]. However, the exact manifestation of "order" in terms of protein secondary and tertiary structure is variable and still under debate for silk fibres [19]; as such, we use the terminology of "order" and "disorder" in the context of this work as a two-parameter description of

* Corresponding author. Present address: The University of Sheffield, Department of Materials Science and Engineering, Sheffield S1 3JD, UK. Tel.: +44 114 222 5477.
E-mail address: christopher.holland@sheffield.ac.uk (C. Holland).
[1] Present address: Beihang University, School of Materials Science and Engineering, International Research Center for Biological and Nature-Inspired Materials, Beijing, 100191, China.

http://dx.doi.org/10.1016/j.actbio.2014.09.021
1742-7061/

energy management in a material where different hydrogen bonding states can directly influence mechanical properties.

As detailed conformational structure is not a focus of this work, DMTA has advantages over other spectroscopic techniques (such as small-angle scattering, infrared or nuclear magnetic resonance [23–27]), where structural influences on mechanical properties are inferred. DMTA has the ability to directly probe structural transitions that affect the mechanical properties of the material through changes (peaks) in the loss tangent. The disadvantages of DMTA in turn are that these transitions have to be related back to specific states of matter (amorphous or crystalline) and local chain conformations or intermolecular bond strengths. However, this relationship has been discussed in detail from both an empirical perspective [28] and also using robust structure–property models for the past 40 years [2,17–19,29–32]. Furthermore, it is now possible to relate these DMTA spectra to distinct mechanical property profiles obtained from tensile testing, as we shall demonstrate in this study.

Native silks and RSFs are often composed of the same peptide motifs [11], and hence patterns of structural and property differences between the two resulting fibres might be due to both spinning and processing condition differences. Not a focus here, several studies have shown how RSF can be post-spun processed (termed "post-processed") in a variety of ways, using chemical or isothermal treatment or applying postdraw, which influences the structures present [11,12,33–38]. Other studies make the important link between the treatment, the mechanical properties and the protein structure [9,16,39–41]. To date, artificially spun silks (unless considerably post-processed) are unable to match their natural counterparts [42]. This is most likely because the initial spinning and the common post-processing conditions used lead to dissimilar supra-molecular structures [42].

This study presents forced reeled silks as an ideal study material to help inform about the differences between natural cocoon silk and unnaturally spun RSF, providing insights into the relative importance of spinning and post-processing conditions. Fibres drawn by forced reeling originate from natural silk dope and are spun in vivo but, we assume, under somewhat "unnatural" (i.e. semi-natural) spinning conditions since the silk fibre is pulled directly from the spinnerets [43–45]. Unlike naturally spun silks, processing conditions can be applied to forced reeled silks during spinning [43,45,46]. Studying the relationship between the properties and degree of order (modelled as the state of hydrogen bonding) of these silks produced under a range of conditions might help to explore the importance of spinning by establishing a full picture of the performance range of such materials. This, in turn, can help us establish a link between naturally, semi-naturally and artificially spun silk fibres based on native dopes and fibres spun from artificial RSFs.

Since processing conditions can be manipulated during reeling, forced reeled silks can have an impressive range of properties compared to naturally spun silks [43,45,46]. Under experimental reeling conditions, forced reeled silk variability between worms can be controlled by removing behavioural application of load by the silkworm, which can affect the silk's mechanical properties [45,47]. Silkworm paralysis removes this behavioural variation [45], which makes it possible to explore the performance range of the forced reeled silks through manipulation of processing conditions.

Reeling speed is the best-studied processing condition influencing mechanical properties through affecting protein-chain order during reeling [43,46]. A recent paper demonstrates how reeling speeds comparable to the average natural spinning speed can give greater toughness, concluding that reeling speed somehow affects structure and morphology of the fibre [45]. Of course, post-processing conditions during reeling, such as postdraw (stretching the fibres during reeling) or wet-reeling (dipping the silk through water during reeling), would also be expected to create additional order [48]. Adding tension to the fibre before it is fully set creates stress-induced molecular alignment [49], allowing hydrogen bonding during drying to "lock" the order into place [48]. Indeed, in spider spinning, such post-processing additions affect the mechanical properties by increasing the order within the fibre [48,50]; this is also seen in synthetic polymer spinning [51–54]. To further increase the degree of molecular order in a finished silk fibre, the post-processing conditions of parameters like temperature, stress and solvation would need to exceed the yield point or glass transition temperature to allow macromolecular mobility [18].

This study aims to use the scope of properties produced by forced reeled silks to infer the relative importance of spinning and post-processing conditions, through comparison to naturally and unnaturally spun silk fibres. Since naturally spun silks have the least variable and most desirable properties, comparison to naturally spun silks is our main focus in this study. The mechanical property differences are explored using a combination of thermogravimetric analysis (TGA) and DMTA temperature scans to infer the degree of order and local states of bonding in the polymer structure. We investigate how processing conditions can influence the envelope of forced reeled silk properties and the degree of order [2,29,30] by examining the effects of reeling speed, and post-processing conditions such as degree of postdraw, specimen tension and storage conditions. The resulting insights can be interpreted in the context of all silk-derived materials from natural to synthetic.

2. Methods

2.1. Materials

Final instar *B. mori* silkworms were reared on a mulberry diet. Worms were stored in laboratory conditions until they started spinning (20 °C, 40% relative humidity, RH). All worms were immobilized for forced reeling using a synthetically produced, but naturally occurring, paralysis peptide, sourced from Activotec, Cambridge (peptide sequence ENFVGGCATGFKRTADGRCKPTF). The peptide is injected into the haemolymph, as described elsewhere [45]. Worms were then suspended from a holder using tape around their body (Supplementary Fig. S1). The paralysis reduces the effect of silkworm behaviour on properties, so increases the reproducibility between different worms [45]. Being invertebrates, all silkworms were handled according to local laboratory risk assessments/institutional ethical guidelines and do not currently fall under regulation by the UK Home Office or EU legislation.

The reeling conditions and specimen storage details are given in Table 1. All non-postdrawn silks were reeled in air straight onto a motorized spool at the stated reeling speed [45]. Postdrawn silks were run through a water bath via a Teflon-coated guide before winding through motorized wheels, which applied a controlled postdraw. A water bath is used as water acts as a plasticizer, thus reducing the likelihood of breaking and increases the likelihood of macromolecular movement during applied postdraw. The first wheel was set to the reeling speed of 20 mm s^{-1}. The second wheel was placed at different distances away from the first wheel. The silk was collected onto a motorized spool for collection, travelling at the same speed as the second wheel. Dry storage silks were reeled onto a spool in laboratory conditions and then kept in sealed low humidity conditions (5% RH) until the fibres were mounted and tested in laboratory conditions.

Naturally spun silk specimens were unravelled from a cocoon onto a spool. Specimens were collected from within over 500 m of the unravelled silk length, which showed consistent properties

Table 1
Reeling and silk storage conditions for the non-postdrawn and postdrawn (PD) forced reeled silks.

Forced reeling processing	No. of specimens tensile tested	Initial reeling speed (mm s^{-1})	Postdraw applied[a]	Distance between postdraw wheels (mm)	Spool storage	Specimen tension	DMTA analysis[b]
No postdraw	N/A	18			lab	tension	120 °C annealing
No postdraw, dry-storage	15	20			5% RH storage conditions	tension	180 °C annealing; temperature scan
No postdraw slack	7	20			lab	slack	temperature scan (plus TGA)
No postdraw tension	7, 5, 5, 5	6, 15, 20, 25			lab	tension	temperature scan (exception: 20 mm s^{-1})
PD × 1.1 slow	7	20	×1.1 (±0.4)	226	lab	tension	
PD × 1.16 fast	7	20	×1.16 (±0.4)	99	lab	tension	120 °C annealing
PD × 1.16 slow	5	20	×1.16 (±0.4)	226	lab	tension	temperature scan

The reeling speed was kept the same between forced reeled silks for consistency and postdraw was chosen based on practical ratios that were possible above yield without breaking within the error margin of the set-up. For details on the DMTA parameters, see Section 2.4.
[a] Error on the postdraw applied comes from the error in the measured wheel diameter, which is used to work out the circumference and speed of the rotating wheel.
[b] Where number of specimens tested is two or three per type of scan.

[45]. Some tests used degummed naturally spun silk; the degumming process is described in detail elsewhere [24]. The RSF fibres used for the DMTA test were kindly supplied by Wang Qin at Fudan University. The RSF solution was obtained using the same method as Wang et al. [55] and the fibres were obtained through wet-spinning similar to the methods used in Yan et al. [56]. The RSF stress–strain curves and DMTA profiles are provided for reference only, to allow the properties of forced reeled silks to be compared within the context of natural and unnaturally spun silks.

2.2. Thermogravimetric analysis

Aluminium pans and 100 µl crucibles were pre-tared on the thermogravimetric analyser balance prior to adding the specimen (TA Instruments Q500 thermogravimetric analyser). Approximately 0.3 mg (3 m) of silk was then cut from a spool and carefully transferred into the aluminium pan. The specimen was then heated at a rate of 3 °C min^{-1} from ambient temperature to 300 °C in nitrogen gas flowing through the thermogravimetric analyser furnace at a rate of 100 cc min^{-1}.

2.3. Tensile testing

Fibres were mounted under tension into 10 mm gauge length cardboard frames for tensile testing (5 N load cell, model 5512, Instron, UK). The numbers of specimens tensile tested are given in Table 1. Specimens were pulled apart in laboratory conditions (40% relative humidity, 21 °C) at a controlled strain rate of 40% min^{-1} until broken; only specimens that broke in the middle were used. The load–extension data were analysed using a Microsoft Excel macro and figures were drawn using Origin Software (OriginPro8).

Quasi-static tensile tests were also performed using the DMTA (TA Q800) in controlled-force mode at room temperature. Dry nitrogen purge was applied for 15–30 min to remove the excess moisture of the specimen after it was loaded onto the clamps. A force-ramp rate of 0.1 N min^{-1} was applied for all forced reeled *B. mori* silks, with two or three specimens being tested from each processing treatment.

The cross-sectional area is measured by gluing silk specimens to solder with superglue, as described in detail elsewhere [45]. Silk fibres were then transversely sectioned, digested in protease for 24 h and imaged in a scanning electron microscope. Pictures were analysed using ImageJ software (NIH). The average area is applied to the specimens used in the tensile tests [45].

Non-parametric statistics were performed using Minitab v.8 software, being the most suitable tests for low specimen numbers ($n < 30$). A Moods sign test was used, which does not assume equal variance.

2.4. Dynamic mechanical thermal analysis

All the dynamic mechanical thermal tests were performed on TA Q800 under DMTA multi-frequency strain mode. The parameters kept as constants were: (i) temperature ramp rate at 3 °C min^{-1}; (ii) frequency at 1 Hz; and (iii) dynamic strain at 0.1%. The selection of these constant parameters was based on the most common polymer testing procedure as well as a compromise between the length of test time and data quality. A preload force equivalent to 50 MPa stress was applied in order to keep the fibre tested in tension throughout the dynamic oscillation. Further details of the background of the technique can be found in Guan et al. [17–19].

Two types of temperature scans were conducted for forced reeled silks: first, a full-range temperature scan from −100 °C to +270 °C ("temperature scans"; see Table 1 for the silks tested), and secondly, cyclical temperature scans, with the first ramp up to +120 °C or +180 °C, abbreviated as 120 °C annealing and 180 °C annealing, respectively (see Table 1 for the silks tested).

3. Results

3.1. Thermal decomposition and structure

Forced reeled silks are compared to naturally spun silks in the thermogravimetric analyser, which provides insights into the different structures present given their apparently similar spinning conditions (Fig. 1). The water content of the forced reeled silks (three repeats, slack storage) was higher than naturally spun and degummed naturally spun silk (ca. 7, 6 and 4.5%, respectively) calculated from the weight loss up to 100 °C. Although these differences are small, the repeatability is good: several meters of silks were tested and the storage conditions prior to testing were identical, so any differences can attributed to the polymer structure, averaged over several meters of silk fibre. Since water is associated with hydrogen bonding to disordered silk [17], this suggests that forced reeled silks are intrinsically more disordered, with larger amorphous fractions (tested later in Sections 3.2 and 3.4). The earlier onset of thermal decomposition in forced reeled silks also supports their being more amorphous. These observations imply that

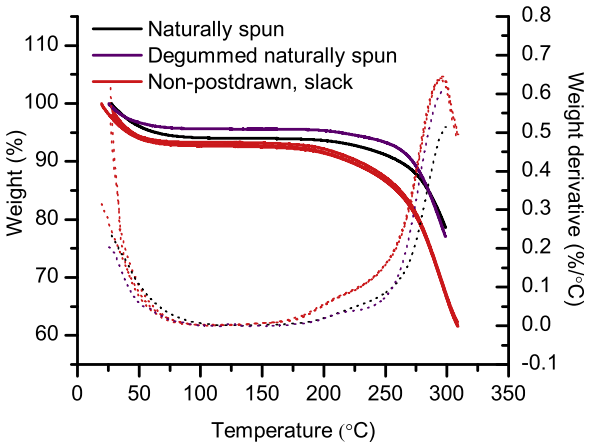

Fig. 1. TGA plot of 3 m of naturally spun (black), degummed naturally spun (purple) and three repeats of a non-postdrawn silk (slack; red) forced reeled silks. The solid lines give the weight loss over temperature and the dotted lines give the weight derivative over temperature.

forced reeled silks are more disordered and have lower values of the glass transition temperature, T_g, which would be due to the higher vibrational energy of the less rigidly bonded chain backbone [17,57].

3.2. Reeling speed and structure

The differences between forced reeled and naturally spun silks were further explored in terms of the influence of the applied processing conditions on the forced reeled silk, here reeling speed. Previous results have shown that the mechanical properties of forced reeled silks are toughest (integrating stress and strain) at the reeling speed closest to the naturally spun reeling speed (ca. 10 mm s^{-1}) [45]. This is confirmed by the data shown in Fig. 2a, where stress–strain curves at three reeling speeds, 6, 15, and 25 mm s^{-1}, are compared with naturally spun cocoon silk. Silks reeled at a speed of 15 mm s^{-1} displayed average toughness closest to that of naturally spun silks, albeit with slightly higher variability (naturally spun mean ± standard deviation of 63.9 ± 8.8 J cm^{-3} (n = 6), 15 mm s^{-1} forced reeled 100.0 ± 20.8 J cm^{-3} (n = 5).

Even more pronounced than the data shown in Fig. 1, using DMTA forced reeled silks showed thermomechanical behaviour that was significantly different from that of naturally spun silks, with high variability and higher loss tangent peaks at lower temperatures (Fig. 2b). In general, stronger hydrogen bonding in more ordered structures would give higher peak temperatures [17]. Recent work by Guan and collaborators has shown that each loss peak is caused by the glass transition of a specific silk structure, each with different numbers and combinations of hydrogen bonds between the different chemical groups, such as the main chain amide groups or the side-chain –OH groups of serine peptides [2,17,29,30]. The main non-natural loss peak at 175 °C is assigned to the characteristic glass transition temperature of the highly disordered structure of RSF silk [11,17]. The structure associated with this loss peak has two hydrogen bonds per peptide segment in a random disordered configuration [17]. Importantly, the strong loss peak at 120 °C has not previously been observed during DMTA analysis of silk fibres. This peak is not due to water, as the TGA profile did not show weight loss at this temperature (Fig. 1). Calculations using the Guan model [17] suggest that the number of hydrogen bonds for this peak is reduced to one per segment within the disordered structure.

The general conclusion from Figs. 1 and 2 suggests that forced reeled silks are more disordered than naturally spun silks, regardless of the applied processing condition of reeling speed. However, despite this difference, at reeling speeds closer to the average natural spinning speed (15 mm s^{-1}), the total energy required to break the hydrogen bonded structure (a measure of material toughness) was highest, even above that of naturally spun silk (Fig. 2a).

3.3. Using processing conditions to manipulate mechanical properties

It emerged from our TGA and DMTA experiments that forced reeled silks have intrinsically different mechanical and structural properties compared to naturally spun silks. As previously stated, mechanical properties in fibres can be manipulated post-spinning by applying processing conditions to influence the properties, as illustrated in Fig. 3. Here, a consistent reeling speed of 20 mm s^{-1} was chosen for comparison between samples.

Supporting the data in Fig. 2, naturally spun silks had relatively low sample variability compared with the range of forced reeled examples (Fig. 3a). As the methods for mounting and testing the fibres are the same for both naturally spun and forced reeled silks, this leads to the conclusion that the forced reeling processing treatment introduces this variability. The general conclusion for forced reeled silks would propose that more/greater postdraw and higher stretch rate lead to the strongest silks; however, these manipulations were accompanied by greater specimen variability in the post-yield stress–strain profile. These data also indicate

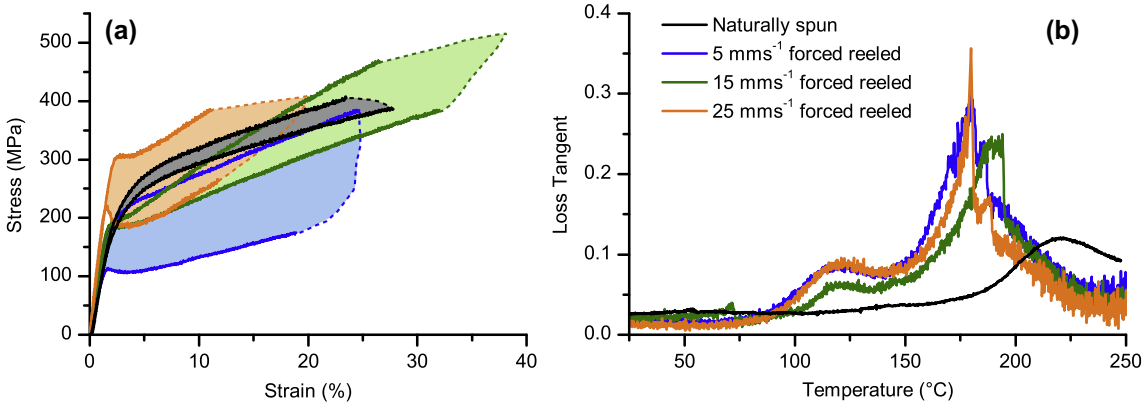

Fig. 2. Differences between forced reeled silks reeled at different speeds: (a) stress–strain profile showing the envelope of properties per material type and (b) loss tangent. Blue denotes 6 mm s^{-1}, green 15 mm s^{-1}, orange 25 mm s^{-1} and black denotes naturally spun silk, where curves shown are from one fibre, chosen from three repeats of the same silk type.

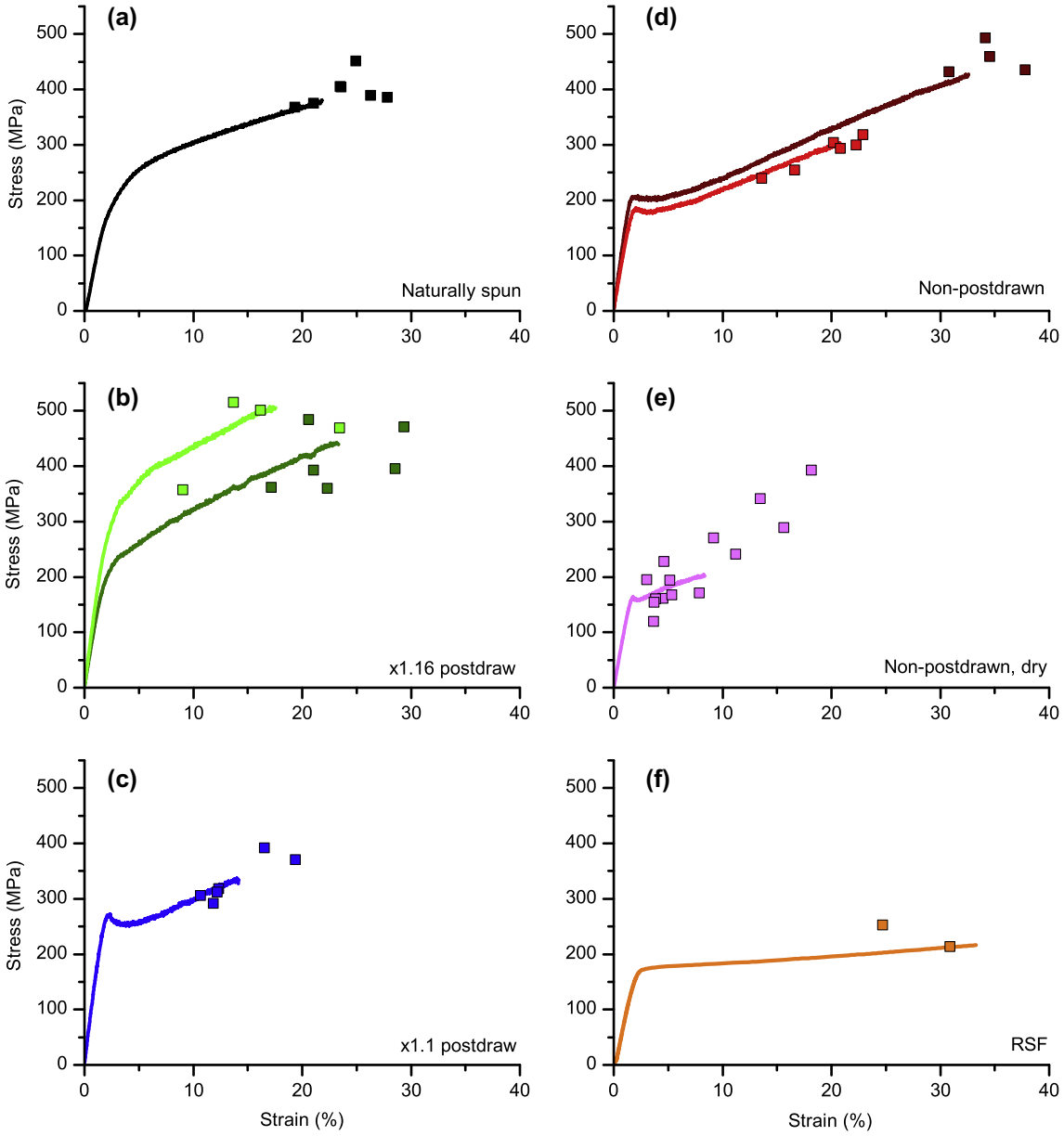

Fig. 3. Stress–strain plots in order of decreasing strength: (a) naturally spun (black); (b, c) postdrawn silks: ×1.16 slow and fast (light and dark green respectively) and × 1.1 slow (blue); (d, e) non-postdrawn silks: tension and slack (dark red and red respectively), and dry storage (5% RH, pink); (f) reference RSF silk (orange). All forced reeled silks are reeled at a consistent speed (here 20 mm s^{-1}) out of a paralysed silkworm, reducing the variability between worms. Scatter points give the breaking points of other specimens tested from the same treatment (for details see Table 1). Specimens on the same plot are comparable as they are from the same worm. The strength reduces down the figure on average.

sensitivity to specimen storage conditions such as silk tension (Fig. 3d) and specimen storage humidity (Fig. 3d and e; mainly affecting specimen consistency). Differences between forced reeled silks are expected to be minimal due to the paralysis condition [45].

Higher postdrawn specimens (×1.16 in Fig. 3b) displayed higher average failure stresses. This might be due to the higher fibre stiffness caused by higher molecular orientation, which in turn would be enhanced by the increased stretching force and higher stretch rate [9,18]. Interestingly, the postdraw affected not only the mechanical properties, but also the fibre cross-sectional areas. Reeling from the same worm and applying the same amount of stretch (×1.16), allowing less time to respond to this stretch (i.e. faster stretch rate), led to a significant decrease in fibre cross-sectional area (from 2.60×10^{-4} mm^2 to 1.44×10^{-4} mm^2; $p < 0.01$, Moods sign test).

Additionally, the postdrawn specimens showed high variability throughout the stress–strain profile, resulting in variability in both stress and strain to failure. This is in contrast to the non-postdrawn specimens in Fig. 3d and e, which followed more consistent stress–strain contours and only varied in their failure points along the contours.

Not found in the high postdrawn specimens (Fig. 3b) nor in naturally spun silks (Fig. 3a), the post-yield plateau in stress seen immediately after yield indicates molecular chain elongation. This is probably associated with plastic flow, as coiled molecules relax through yield until they are stretched sufficiently to sustain the applied load with the equilibrium post-yield modulus [41].

Maintaining tension in the non-postdrawn specimens gave consistently high failure stresses and strains, thereby producing the highest toughnesses seen in any of the fibres drawn. These fibres

were the most similar to naturally spun threads, albeit with an increased post-yield plastic flow in the disordered structures resulting in slightly higher energy uptake, i.e. the area under the stress–strain curve.

Storing the non-postdrawn specimen under dry conditions induced a different kind of variability. Many of these fibres were slightly embrittled by the dry conditions, with associated low failure stress near the yield stress [58]. Water acts as a plasticizer for silk by generating lower temperature relaxation processes that can promote ductility, as can be seen in Figs. 4 and 5 and in the discussion of dynamic mechanical properties [17]. Alternative explanations to the effect of dry-storage include the embrittlement of the sericin binder coating on the fibres, which weakens the whole fibre structure when cracks are initiated in the sericin layer and propagate through the whole fibre [59,60]. Equally, cracks in the sericin layer may lead to brin separation, as seen in previous studies testing cocoon silks in different humidities, which will further increase variability by affecting core fibroin–water interactions [60].

A disordered (largely amorphous) RSF fibre is shown for reference in Fig. 3f. These fibres have little or no post-yield modulus due to their structural morphology. In contrast with native silks, they have larger and more widely distributed ordered regions in the amorphous matrix [11], leading to little contribution of the ordered regions to mechanical performance post-yield.

3.4. Processing conditions and structure

We must ask to what extent (and how) such post-processing conditions affect the amount of structural disorder of forced reeled silks. Fig. 4a presents the temperature scans of two non-annealed and non-postdrawn and one non-annealed but postdrawn forced reeled silk, with naturally spun silk for reference (stress–strain profiles of annealed and non-annealed silks are given in Supplementary Fig. S2). The data of Fig. 2b suggested that all forced reeled silks have complex combinations of partially disordered structures in the fibroin that was introduced by the forced reeling spinning process. Post-treatment could only partially compensate for this increased and variable disorder. Here postdrawing had the strongest effect yet retained strong evidence of multiple types of disordered structure. The highest level of disorder was seen in the non-postdrawn specimens that had been slack-stored before measuring.

In contrast, the greatest order seen in forced reeled silks emerged following annealing to 180 °C (Fig. 4b). Annealing to 180 °C removed small loss peaks associated with water below 100 °C and most of the higher temperature glass transition peaks below about 200 °C, leaving a higher temperature peak comparable to a peak in non-annealed, naturally spun silkworm silk. We suggest that annealing creates stronger bonding as disordered structures are irreversibly stretched under slight mechanical load [17]. Over the temperature range for the annealing scan, this would eventually lead to the formation of the most strongly bonded disordered structure possible in a particular specimen. Importantly, this suggests that thermal treatment under mechanical load would be the most effective way to create ordered structures in a silk. Not surprisingly, this feature is similar to the common practice of annealing synthetic polymer fibres such as PET under load at elevated temperatures in order to increase the orientation and crystal fractions, which in turn increases stiffness and strength [61].

Post-processing conditions therefore influence the properties and structures of forced reeled silks to cover a spectrum of disorder, ranging from the disordered artificially spun RSF to the more ordered naturally spun silks (Fig. 5). For non-annealed silk, peaks associated with more water between −60 and +60 °C indicate more disorder and were highest for non-postdrawn silks, lower for postdrawn silks and lowest for naturally spun silks; no RSF was tested in annealing mode (Fig. 5a). Annealing to 120 °C removed the loss peaks under 100 °C by removing the water from the silk specimens (Fig. 5a). Similar annealing effects have been observed and explained likewise in soy protein [57].

Following 120 °C annealing, the most disordered *Bombyx*-derived protein was RSF. The large RSF loss peak at 175 °C has been assigned to the highly disordered macromolecular structure, which shows the largest area under the loss peak due to the high contribution of disordered structure [2,17,29–32]. These structures are caused by the formation of solid silk from solutions made by the chaotropic medium of aqueous concentrated lithium bromide solution [11]. The non-postdrawn silk loss peak was the least ordered of our forced reeled silks and was most similar to the RSF, suggesting that the non-crystalline fraction is likely to be highly disordered with a structure analogous to RSF.

The postdrawn forced reeled specimen showed an interesting rapid change around 175 °C. This sample loss tangent trace started out like an RSF structure peak but then rapidly changed to resemble a more ordered structure similar to a natural silk. This specimen further supports the assertion that discrete loss peaks in the loss tangent profile of silks are associated with specific hydrogen bonded structures.

Furthermore, this result implies that, under certain conditions of forced reeling, hidden functionality can be locked into the fibre and later released under certain annealing conditions. In the

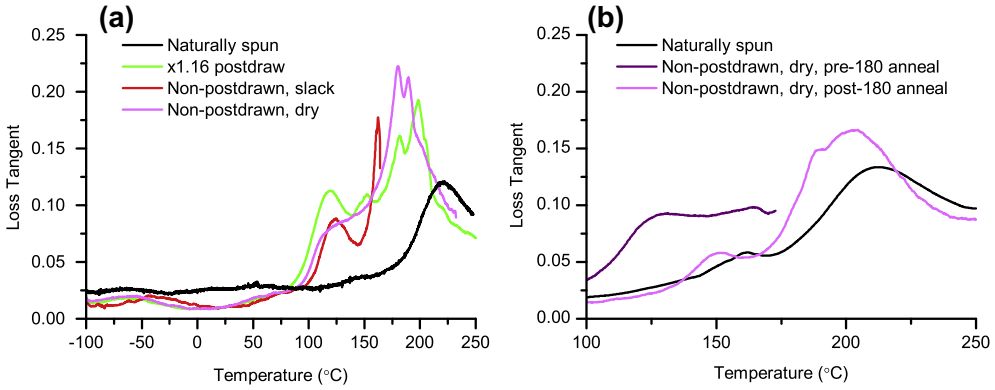

Fig. 4. Loss tangent profiles of various forced reeled *B. mori* silks from three different reeling conditions: (a) ramp straight up (no annealing) for slack-stored non-postdrawn silk (red; broke midway through sampling), dry-storage non-postdrawn silk (5% RH, pink) and × 1.16 slow postdrawn silk (light green); (b) the loss tangent profile of dry-storage non-postdrawn silk (5% RH) before (purple) and after (pink) annealing to 180 °C [17], in comparison with standard naturally spun silk (black). Curves shown are from one fibre, chosen from three repeats of the same silk type. Full details of the forced reeled silk processing are given in Table 1.

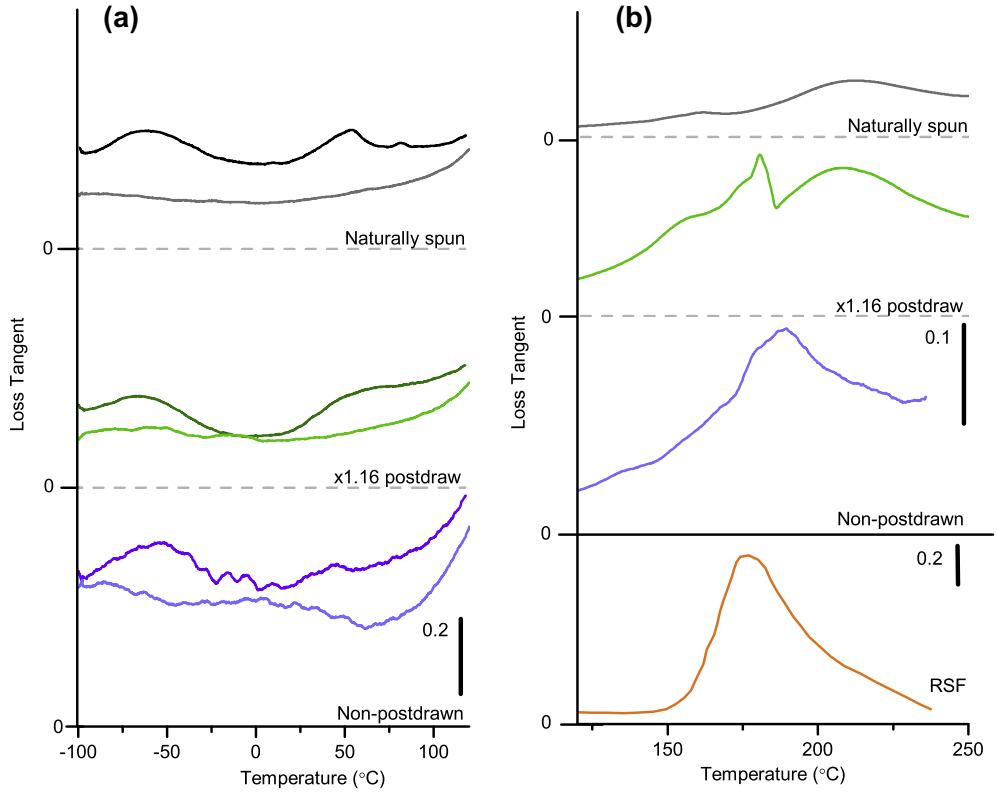

Fig. 5. (a) Loss tangent over temperature pre- and post-120 °C annealing [17] (dark and light respectively) on naturally spun silk (black and grey), postdrawn (×1.16 fast; dark and light green) and non-postdrawn (dark and light purple) forced reeled *B. mori* silks. The bar gives the *y*-axis scale. (b) The post-120 °C annealed loss tangent, including reference RSF (orange). The black bar gives the *y*-axis scale for the top and bottom sections. Curves shown are from one fibre, chosen from three repeats of the same silk type. Further details of the forced reeled silk processing are given in Table 1.

specific bonding arrangement of this postdrawn silk, the structure can clearly be seen to "dynamically" reassemble under specific load and temperature conditions (e.g. change in Fig. 5b, post-yield arrangement in Fig. 3). The specific conditions leading to this dynamic reassembly have not been asserted, but are likely to be linked to the stress and humidity history of the silk [17–19].

4. Discussion

Forced reeled silks were variable in many aspects of their structures and properties, varying more than naturally spun silks and in some cases seemed more akin to derived RSF fibres. Previous work has suggested that such variation in mechanical properties might be attributable to topological "defects" such as surface imperfections present in the silks [44], which may be exacerbated by cross-sectional area measurement and behavioural control of the silk press during non-paralysed reeling [44,45]. This may be the case for certain post-processing conditions, such as dry storage, which leads to sericin cracking when the fibre is under tension, leading to brin separation or crack propagation [60]. In more general terms, our new data in combination suggest that this variation may be attributed to the amount of different disordered protein structures present, as revealed by DMTA. The exact manifestation of the order and disorder in terms of protein tertiary packing is an area of contestation that requires further study, but this by no means diminishes the power of DMTA to resolve structural differences and the impact these have on the mechanical properties of silk fibres [19]. The precise mechanism by which the differences in structures arise between naturally spun and semi-naturally spun forced reeled silks is currently unknown, but is likely to be a product of both behavioural and physiological control exerted by the silkworm during spinning and processing.

Behavioural control in this work was experimentally manipulated by use of a paralytic agent, which is believed to inhibit muscular control around the spinning apparatus, specifically the silk press [45]. This inhibition prevents the animal from using its behaviour to fine-tune the ratio of applied force and reeling rate during fibre production. A lack of feedback and control during silk production could propagate rheological flow instabilities in the silk dope in the duct, as well as preventing any post-spinning postdraw of fibres.

Furthermore, forced reeling may impact the silkworms' physiological control, i.e. the exposure of the dope to chemical processing in the duct (changes in pH and ions), known to affect silk's self-assembly properties [62–66]. Recent work suggests that specific chemically induced links between terminal groups on the protein chains might allow the flow field in the duct to stretch the macromolecules into an aligned structure that in turn promotes structural order and inter-chain hydrogen bonding [67,68].

Identifying the biological origin of property variability in our forced reeled silks is far beyond the scope of the current work, but the tools presented here, in cooperation with other structural analysis tools, such as X-ray scattering, Fourier transform infrared and Raman spectroscopy, will allow these origins to be explored in the future.

A fibre's stress–strain profile ultimately (and arguably) determines its application and function. Concerning mechanical properties, we have shown that postdrawn forced reeled silks are able to achieve higher strength, albeit at the cost of extensibility, toughness and consistency. The toughest fibres were the non-postdrawn forced reeled silks under specific storage conditions (tension and humid). Thermal stability analysis using TGA and DMTA loss spectra both showed that naturally spun silks showed the highest degree of order, and that the forced reeled silk properties are

controlled by the fraction and type of disorder. This suggests that forced reeling introduces disorder into the fibre that can only be fully addressed with post-reeling processing conditions such as thermal treatment under load. This would permit precise control of the structure and properties of semi-natural forced reeled silk fibres for bespoke applications.

5. Conclusions

We have shown that, with controlled forced reeling of *B. mori*, one is able to produce fibres with a wide range of mechanical properties, which is beginning to make clear links between natural and artificial silk in terms of spinning and processing conditions. Moreover, our data demonstrate that DMTA analysis on silk fibres is not only useful as a tool to assess the quality of a fibre [17], but can also quantitatively assess a fibre's potential for improvement through post-spin modification, regardless of the fibre's origin or processing history. More specifically, our data elucidate the range of properties available to *B. mori* silks and silk-based fibres, which in turn has important implications for their industrial application.

6. Supplementary material available

Two supplementary figures accompany this manuscript. Fig. S1 shows the experimental set-up for the forced reeling silkworms. A silkworm is attached onto a pole (a) using tape around its body between the "thoracic" and "pseudo" feet (b). The silk is attached onto a rotating cylindrical spool (c), which is controlled by a motor and moved by hand to collect the silk along the spool. Fig. S2 shows the stress–strain curves before (darker, open scatter points) and after (lighter, filled scatter points) 120 °C annealing for naturally spun (black/grey), postdrawn (×1.16 fast; greens) and non-postdrawn silk (purples)). Scatter points give the break points of repeats of the same silk types.

Acknowledgements

The authors thank Nick Hawkins for running specimens on the TGA and DMTA and Sophie Scott for the help reeling the silkworms. The authors also thank Wang Qin from Fudan University for providing RSF fibre specimens. For funding we thank The Leverhulme Trust (F/08705/D), the US Air Force Office of Scientific Research (FA9550-12-1-0294), the European Research Council (SP2-GA-2008-233409), Chinese Ministry of Education – University of Oxford Scholarship (for J.G.) and the EPSRC (EP/K005693/1).

Appendix A. Supplementary data

Supplementary data associated with this article can be found, in the online version, at http://dx.doi.org/10.1016/j.actbio.2014.09.021.

Appendix B. Figures with essential colour discrimination

Certain figures in this article, particularly Figs. 1–5 are difficult to interpret in black and white. The full color images can be found in the on-line version, at http://dx.doi.org/10.1016/j.actbio.2014.09.021.

References

[1] Craig C. Evolution of arthropod silks. Annu Rev Entomol 1997;42:231–67.
[2] Porter D, Vollrath F. Silk as a biomimetic ideal for structural polymers. Adv Mater 2009;21:487–92.
[3] Chen F, Porter D, Vollrath F. Structure and physical properties of silkworm cocoons. J R Soc Interface 2012;9:2299–308.
[4] Perez-Rigueiro J, Elices M, Llorca J, Viney C. Effect of degumming on the tensile properties of silkworm (*Bombyx mori*) silk fiber. J Appl Polym Sci 2002;84:1431–7.
[5] Jin HJ, Kaplan DL. Mechanism of silk processing in insects and spiders. Nature 2003;424:1057–61.
[6] Holland C, Terry AE, Porter D, Vollrath F. Natural and unnatural silks. Polymer 2007;48:3388–92.
[7] Zhu ZH, Ohgo K, Asakura T. Preparation and characterization of regenerated *Bombyx mori* silk fibroin fiber with high strength. Express Polym Lett 2008;2:885–9.
[8] Tao H, Kaplan DL, Omenetto FG. Silk materials - a road to sustainable high technology. Adv Mater 2012;24:2824–37.
[9] Yin J, Chen E, Porter D, Shao Z. Enhancing the toughness of regenerated silk fibroin film through uniaxial extension. Biomacromolecules 2010;11:2890–5.
[10] Altman H, Diaz F, Jakuba C, Calabro T, Horan RL, Chen JS, et al. Silk-based biomaterials. Biomaterials 2003;24:401–16.
[11] Yuan QQ, Yao JR, Huang L, Chen X, Shao ZZ. Correlation between structural and dynamic mechanical transitions of regenerated silk fibroin. Polymer 2010;51:6278–83.
[12] Motta A, Fambri L, Migliaresi C. Regenerated silk fibroin films: thermal and dynamic mechanical analysis. Macromol Chem Phys 2002;203:1658–65.
[13] Magoshi J, Magoshi Y. Physical properties and structure of silk 2. Dynamic mechanical and dielectric properties of silk fibroin. J Polym Sci Part B: Polym Phys 1975;13:1347–51.
[14] Tsukada M, Freddi G, Kasai N, Monti P. Structure and molecular conformation of tussah silk fibroin films treated with water–methanol solutions: dynamic mechanical and thermomechanical behavior. J Polym Sci Part B: Polym Phys 1998;36:2717–24.
[15] Kweon HY, Um IC, Park YH. Thermal behavior of regenerated *Antheraea pernyi* silk fibroin film treated with aqueous methanol. Polymer 2000;41:7361–7.
[16] Yang Y, Chen X, Shao ZZ, Zhou P, Porter D, Knight DP, et al. Toughness of spider silk at high and low temperatures. Adv Mater 2005;17:84–8.
[17] Guan J, Porter D, Vollrath F. Thermally induced changes in dynamic mechanical properties of native silks. Biomacromolecules 2013;14:930–7.
[18] Guan J, Porter D, Vollrath F. Silks cope with stress by tuning their mechanical properties under load. Polymer 2012;53:2717–26.
[19] Guan J, Vollrath F, Porter D. Two mechanisms for supercontraction in *Nephila spider* dragline silk. Biomacromolecules 2011;12:4030–5.
[20] Magoshi J, Nakamura S. Studies on physical-properties and structure of silk – glass-transition and crystallization of silk fibroin. J Appl Polym Sci 1975;19:1013–5.
[21] Magoshi J, Magoshi Y, Nakamura S. Physical properties and structure of silk 3. Glass-transition and conformational changes of tussah silk fibroin. J Appl Polym Sci 1977;21:2405–7.
[22] Nakamura S, Saegusa Y, Yamaguchi Y, Magoshi J, Kamiyama S. Physical properties and structure of silk. X1. Glass-transition temperature of wild silk fibroins. J Appl Polym Sci 1986;31:355–6.
[23] Dicko C, Kenney JM, Vollrath F, Andrey Kajava JMSaDADP. Beta-Silks: Enhancing and Controlling Aggregation. New York: Academic Press; 2006. p. 17–53.
[24] Greving I, Dicko C, Terry A, Callow P, Vollrath F. Small angle neutron scattering of native and reconstituted silk fibroin. Soft Matter 2010;6:4389–95.
[25] Mo C, Holland C, Porter D, Shao Z, Vollrath F. Concentration state dependence of the rheological and structural properties of reconstituted silk. Biomacromolecules 2009;10:2724–8.
[26] Riekel C, Madsen B, Knight D, Vollrath F. X-ray diffraction on spider silk during controlled extrusion under a synchrotron radiation X-ray beam. Biomacromolecules 2000;1:622–6.
[27] Asakura T, Suzuki Y, Nakazawa Y, Holland GP, Yarger JL. Elucidating silk structure using solid-state NMR. Soft Matter 2013;9:11440–50.
[28] McCrum NG, Read BE, Williams G. Anelastic and dielectric effects in polymeric solids. London: John Wiley & Sons; 1967.
[29] Vollrath F, Porter D. Spider silk as a model biomaterial. Appl Phys A Mater 2006;82:205–12.
[30] Vollrath F, Porter D. Spider silk as an archetypal protein elastomer. Soft Matter 2006;2:377–85.
[31] Porter D. Group Interaction Modelling of Polymer Properties. New York: Marcel Dekker; 1995.
[32] Porter D, Gould PJ. Predictive nonlinear constitutive relations in polymers through loss history. Int J Solids Struct 2009;46:1981–93.
[33] Hu X, Kaplan D, Cebe P. Dynamic protein-water relationships during beta-sheet formation. Macromolecules 2008;41:3939–48.
[34] Hu X, Kaplan D, Cebe P. Determining beta-sheet crystallinity in fibrous proteins by thermal analysis and infrared spectroscopy. Macromolecules 2006;39:6161–70.
[35] Um IC, Kweon HY, Park YH, Hudson S. Structural characteristics and properties of the regenerated silk fibroin prepared from formic acid. Int J Biol Macromol 2001;29:91–7.
[36] Jeong L, Lee KY, Liu JW, Park WH. Time-resolved structural investigation of regenerated silk fibroin nanofibers treated with solvent vapor. Int J Biol Macromol 2006;38:140–4.
[37] Zhou L, Chen X, Shao ZZ, Huang YF, Knight DP. Effect of metallic ions on silk formation the mulberry silkworm, *Bombyx mori*. J Phys Chem B 2005;109:16937–45.

[38] Lu Q, Zhu HS, Zhang CC, Zhang F, Zhang B, Kaplan DL. Silk self-assembly mechanisms and control from thermodynamics to kinetics. Biomacromolecules 2012;13:826–32.
[39] Jiang CY, Wang XY, Gunawidjaja R, Lin YH, Gupta MK, Kaplan DL, et al. Mechanical properties of robust ultrathin silk fibroin films. Adv Funct Mater 2007;17:2229–37.
[40] Zhou GQ, Shao ZZ, Knight DP, Yan JP, Chen X. Silk fibers extruded artificially from aqueous solutions of regenerated *Bombyx mori* silk fibroin are tougher than their natural counterparts. Adv Mater 2009;21:366–70.
[41] Wang Y, Porter D, Shao ZZ. Using solvents with different molecular sizes to investigate the structure of *Antheraea pernyi* silk. Biomacromolecules 2013;14:3936–42.
[42] Vollrath F, Porter D, Holland C. There are many more lessons still to be learned from spider silks. Soft Matter 2011;7:9595–600.
[43] Shao ZZ, Vollrath F. Surprising strength of silkworm silk. Nature 2002;418. 741–741.
[44] Perez-Rigueiro J, Elices M, Llorca J, Viney C. Tensile properties of silkworm silk obtained by forced silking. J Appl Polym Sci 2001;82:1928–35.
[45] Mortimer B, Holland C, Vollrath F. Forced reeling of *Bombyx mori* silk: separating behaviour and processing conditions. Biomacromolecules 2013;14:3653–9.
[46] Khan M, Morikawa H, Gotoh Y, Miura M, Ming Z, Sato Y, et al. Structural characteristics and properties of *Bombyx mori* silk fiber obtained by different artificial forcibly silking speeds. Int J Biol Macromol 2008;42:264–70.
[47] Asakura T, Umemura K, Nakazawa Y, Hirose H, Higham J, Knight D. Some observations on the structure and function of the spinning apparatus in the silkworm *Bombyx mori*. Biomacromolecules 2007;8:175–81.
[48] Liu Y, Shao ZZ, Vollrath F. Extended wet-spinning can modify spider silk properties. Chem Commun 2005;19:2489–91.
[49] Knight DP, Knight MM, Vollrath F. Beta transition and stress-induced phase separation in the spinning of spider dragline silk. Int J Biol Macromol 2000;27:205–10.
[50] Liu Y, Shao ZZ, Vollrath F. Relationships between supercontraction and mechanical properties of spider silk. Nat Mater 2005;4:901–5.
[51] Choi KJ, Spruiell JE, White JL. Structure development in biaxially stretched polystyrene film. I. Property-orientation correlation. Polym Eng Sci 1989;29:1516–23.
[52] Tanabe Y, Kanetsuna H. Structure of oriented polystyrene monofilaments and its relationship to brittle-to-ductile transition. J Appl Polym Sci 1978;22:1619–30.
[53] Tanabe Y, Kanetsuna H. Brittle-to-ductile transition based upon amorphous orientation of polystyrene monofilaments. J Appl Polym Sci 1978;22:2707–11.
[54] Zhang XM, Ajji A. Biaxial orientation behavior of polystyrene: Orientation and properties. J Appl Polym Sci 2003;89:487–96.
[55] Wang Q, Yang YH, Chen X, Shao ZZ. Investigation of rheological properties and conformation of silk fibroin in the solution of AmimCl. Biomacromolecules 2012;13:1875–81.
[56] Yan JP, Zhou GQ, Knight DP, Shao ZZ, Chen X. Wet-spinning of regenerated silk fiber from aqueous silk fibroin solution: Discussion of spinning parameters. Biomacromolecules 2010;11:1–5.
[57] Tian K, Porter D, Yao JR, Shao ZZ, Chen X. Kinetics of thermally-induced conformational transitions in soybean protein films. Polymer 2010;51:2410–6.
[58] Reed EJ, Bianchini LL, Viney C. Sample selection, preparation methods, and the apparent tensile properties of silkworm (*B. mori*) cocoon silk. Biopolymers 2012;97:397–407.
[59] Chen FJ, Hesselberg T, Porter D, Vollrath F. The impact behaviour of silk cocoons. J Exp Biol 2013;216:2648–57.
[60] Mortimer B, Drodge DR, Dragnevski KI, Siviour CR, Holland C. In situ tensile tests of single silk fibres in an environmental scanning electron microscope. J Mater Sci 2013;48:5055–62.
[61] Thistlethwaite T, Jakeways R, Ward IM. The crystal modulus and structure of oriented poly(ethylene terephthalate). Polymer 1988;29:61–9.
[62] Dicko C, Vollrath F, Kenney JM. Spider silk protein refolding is controlled by changing pH. Biomacromolecules 2004;5:704–10.
[63] Zhou L, Terry AE, Huang YF, Shao ZZ, Chen X. Metal element contents in silk gland and silk fiber of *Bombyx mori* silkworm. Acta Chim Sin 2005;63:1379–82.
[64] Zhou L, Chen X, Shao Z, Zhou P, Knight DP, Vollrath F. Copper in the silk formation process of *Bombyx mori* silkworm. FEBS Lett 2003;554:337–41.
[65] Peng X, Shao Z, Chen X, Knight DP, Wu P, Vollrath F. Further Investigation on potassium-induced conformation transition of *Nephila spidroin* film with two-dimensional infrared correlation spectroscopy. Biomacromolecules 2005;6:302–8.
[66] Foo CWP, Bini E, Hensman J, Knight DP, Lewis RV, Kaplan DL. Role of pH and charge on silk protein assembly in insects and spiders. Appl Phys A Mater 2006;82:223–33.
[67] Gronau G, Qin Z, Buehler MJ. Effect of sodium chloride on the structure and stability of spider silk's N-terminal protein domain. Biomater Sci 2013;1:276–84.
[68] Gaines WA, Sehorn MG, Marcotte Jr WR. Spidroin N-terminal domain promotes a pH-dependent association of silk proteins during self-assembly. J Biol Chem 2010;285:40745–53.